Solution Processing of Calcium Zirconate Titanates, $Ca(Zr_xTi_{1-x})O_3$: An X-ray Absorption Spectroscopy and Powder Diffraction Study

Jie Xu, Angus P. Wilkinson,* and Sidhartha Pattanaik†

School of Chemistry & Biochemistry, Georgia Institute of Technology, Atlanta, Georgia 30332-0400

Received December 13, 1999. Revised Manuscript Received August 1, 2000

The preparation of perovskite calcium zirconate titanates ($Ca[Zr_xTi_{1-x}]O_3$) via an acetic-acid-modified sol−gel process, two different alkoxide sol−gel routes, and the direct reaction of oxides and carbonates was explored. X-ray absorption spectroscopy measurements on xerogels prepared using alkoxides indicated the presence of zirconium and titanium with coordination numbers >6 and <6, respectively. The use of acetic acid as a modifier changes the local structure around zirconium in the xerogel. A calcium-rich phase was observed at low heat treatment temperatures regardless of the sample preparation route. Many of the initially prepared xerogels contained perovskite and the higher titanium content samples more readily crystallized to perovskite upon heating. None of the processing routes led to the clean formation of perovskite at low temperatures. At intermediate temperatures a fluorite-related phase was always formed in addition to perovskite, and the fluorite-like material transformed to perovskite at higher temperatures. The average composition of the perovskite present in the fluorite−perovskite mixture did not change as more of the fluorite was converted to perovskite by heating, suggesting that the two phases have the same zirconium-to-titanium ratio. The EXAFS analyses indicated that the average Zr−O and Ti−O bond lengths are only weakly dependent upon solid-solution composition, even though the average M−O bond length depends strongly on composition. The EXAFS data also suggest the cation distribution in the solid solution is to some extent dependent upon the sample preparation method.

Introduction

Ca−Zr−Ti−O compositions are primarily of interest because of their use in nuclear waste immobilization[1−4] and microwave dielectric ceramics.[5−9] However, we have studied the $CaZr_xTi_{1-x}O_3$ (CZT) system as a model for $Pb(Zr_xTi_{1-x})O_3$ (PZT) as it can be more readily examined by X-ray absorption spectroscopy (XAS). In PZT, the lead absorbs X-rays strongly at the titanium K-edge. The use of CZT as a model for PZT is reasonable, as evidenced by the similarities in their crystallization when sol−gel processed (see later), but the smaller size of Ca(II) compared to that of Pb(II) and the tendency of Pb(II) to form bonds that are more covalent may lead to differences between the systems. The reported work is focused on understanding how processing chemistry influences the local structure and compositional homogeneity of the products.

Calcium zirconate titanates have been prepared using several solution methods, including alkoxide sol−gel,[1,10,11] oxalate,[1] combustion,[12] and citrate routes.[13] They offer significant advantages over the reaction of $CaCO_3$, TiO_2, and ZrO_2 as the latter requires long reaction times at high temperatures (>1200 °C). Although the sol−gel processing of PZT compositions has been studied extensively, very little work has been done on sol−gel-processed CZT.

We examined four routes for the preparation of CZT: (a) A homogeneous alkoxide sol−gel method, similar to those typically employed for PZT, (b) an inhomogeneous alkoxide sol−gel method, (c) an acetic-acid-modified route,[14] and (d) the direct reaction of oxides. In the homogeneous sol−gel approach, all the starting materials were mixed together at the beginning of the syn-

* To whom correspondence should be addressed.
† Present address: The Consortium for Fossil Fuel Liquefaction Science, University of Kentucky, 533 South Limestone Street, Room 111, Lexington, KY 40506-0043.

(1) Saaverdra, M. J.; Parada, C.; Figueiredo, M. O.; Correa dos Santos, A. *Solid State Ionics* **1993**, *63−65*, 213−217.
(2) Hon, Y.; Shen, P. *Mater. Sci. Eng.* **1991**, *A131*, 273−280.
(3) Shen, P.; Hon, Y. *Mater. Sci. Eng.* **1992**, *A159*, 267−274.
(4) Swenson, D.; Nieh, T.; Fournelle, J. H. *J. Am. Ceram. Soc.* **1998**, *81*, 3249−3252.
(5) Kanai, H.; Furukawa, O.; Abe, H.; Yamashita, Y. *J. Am. Ceram. Soc.* **1994**, *77*, 2620−2624.
(6) Cheon, C.; Kim, J.; Lee, H. *J. Mater. Res.* **1998**, *13*, 1107−1109.
(7) Sivasubramanian, V.; Murthy, V. R. K.; Viswanathan, B. *Jpn. J. Phys.* **1997**, *36*, 194−197.
(8) Kell, R. C.; Greenham, A. C.; Olds, G. C. E. *J. Am. Ceram. Soc.* **1973**, *56*, 352−354.
(9) Hennings, D.; Schreinemacher, H. *Mater. Res. Bull.* **1977**, *12*, 1221−1226.
(10) Piagai, R.; Kim, I.; Park, J.; Kim, Y. *J. Am. Ceram. Soc.* **1998**, *81*, 1361−1364.
(11) Pfaff, G. *Chem. Mater.* **1994**, *6*, 58−62.
(12) Maria, M.; Sekar, A.; Patil, K. *J. Mater. Chem.* **1992**, *2*, 739−743.
(13) Rajendran, M.; Rao, M. S. *J. Mater. Res.* **1997**, *12*, 2665−2672.
(14) Schwartz, R. W. *Chem. Mater.* **1993**, *5*, 511−517.

10.1021/cm990774i CCC: $19.00
Published on Web 10/21/2000

thesis. In the inhomogeneous sol−gel syntheses, $CaTiO_3$ (CT) and $CaZrO_3$ (CZ) precursors were hydrolyzed prior to mixing. The inhomogeneous sol−gel synthesis was performed so that the possibility of controlling a solid-solutions compositional homogeneity could be assessed.

The products from these syntheses were examined by powder X-ray diffraction (XRD), X-ray absorption spectroscopy (XAS), and thermogravimetric/differential thermal analyses (TGA/DTA). XAS is complementary to XRD as it provides information on a material's local structure and it is applicable to both amorphous and crystalline samples.[15,16]

Both PZT and CZT have previously been examined using XAS. The first EXAFS study of $CaTiO_3$ and $CaZrO_3$ was published in 1968.[17] There have been several recent studies of calcium zirconate titanates, including an examination of transuranium elements in $CaTiO_3$,[18] and a study of zirconolite,[19] a component of SYNROC, that examined alpha-decay event damage. For the PZT system there are many XAS papers on either the solution processing of PZT[20−28] or the local structure in highly crystalline samples and how the local structure relates to the phase transitions that are seen in this solid solution.[29−32]

Experimental Section

Sample Preparation. $Ca(NO_3)_2{\cdot}4H_2O$, zirconium butoxide (80% in 1-butanol) and titanium isopropoxide (97%) purchased from Aldrich were used for the CZT sol−gel syntheses. Calcium nitrate was used, rather than a calcium alkoxide, as it was anticipated that the basicity of calcium alkoxides would lead to difficulties during the hydrolysis of the precursor solutions. Solutions of zirconium butoxide (1.11 M) and titanium isopropoxide (1.51 M) in 2-methoxyethanol were prepared and their concentrations determined gravimetrically. The water content of the $Ca(NO_3)_2{\cdot}4H_2O$ was also determined gravimetrically.

A series of 0.03-mol samples of $Ca(Zr_xTi_{1-x})O_3$ (x = 0.00, 0.25, 0.5, 0.75, 1.00) was prepared using a homogeneous sol−gel procedure that will subsequently be referred to as the HSG method. $Ca(NO_3)_2{\cdot}4H_2O$ (7.2 g) was dissolved in 100 mL of 2-methoxyethanol. The solution was refluxed for 1 h and 30 mL of solvent was distilled off to remove water. Stoichiometric amounts of zirconium butoxide and titanium isopropoxide were added. The mixture was again refluxed for an hour and 30 mL of solvent was distilled out. A water:metal alkoxide ratio of 4:1 was used for hydrolysis. Two milliliters of water (0.111 mol) was mixed with 8 mL of 2-methoxyethanol and added drop by drop to the precursors. For $Ca(Zr_{0.5}Ti_{0.5})O_3$ gelation took place after 20 h. All of the gels were vacuum-dried overnight at 200 °C. The xerogels were split into 10 portions. Each was heated at 5 °C/min in air to the final temperature. They were held at that temperature for 5 h.

$Ca(Zr_{0.5}Ti_{0.5})O_3$ samples were prepared by an inhomogeneous sol−gel procedure that will subsequently be referred to as the IHSG method. Two $Ca(NO_3)_2$ solutions (0.015 mol each) were made by dissolving $Ca(NO_3)_2{\cdot}4H_2O$ in 2-methoxyethanol, refluxing for 1 h, and distilling out solvent water mixture. Stoichiometric amounts of zirconium butoxide and titanium isopropoxide were added to the two calcium-nitrate-containing flasks, respectively. The solutions were refluxed for 1 h and then concentrated. Their concentrations were determined gravimetrically to be 0.477 and 0.616 M, respectively. Stoichiometric amounts of the CZ and CT precursors were placed in separate flasks for hydrolysis. A mixture of 1.1 mL of H_2O with 5 mL of 2-methoxyethanol was added drop by drop to the CZ precursor, and a mixture of 1.1 mL of H_2O with 12 mL of 2-methoxyethanol was added to the CT precursor (4:1 water-to-metal alkoxide ratio). These hydrolyses were performed simultaneously. The amount of 2-methoxyethanol in the hydrolysis mixture was selected so that the final concentrations of the CZ and CT sols were both 0.4 M. After 6 h, the CT precursor had a high viscosity while the CZ precursor only showed a slight increase in viscosity. The CZ sol was transferred into the CT flask and all residues were washed into the flask. The mixture was then stirred and dried overnight in a vacuum oven at 200 °C.

$Ca(Zr_{0.5}Ti_{0.5})O_3$ samples were prepared by an acetic-acid-modified procedure, similar to that previously used for PZT,[14] that will subsequently be referred to as the AAM method. First, 0.01 mol of zirconium butoxide and titanium isopropoxide were mixed together. After 5 min, 0.08 mol of acetic acid was added. After an additional 5 min, 10 mL of methanol was added, and 5 min later, 0.02 mol of $Ca(NO_3)_2{\cdot}4H_2O$ was added. The solution was then heated to 85 °C for ≈10 min to dissolve the calcium nitrate. Then, 10 mL of methanol and 5 mL of acetic acid were added. After 2 min, another 10 mL of methanol and 5 mL of acetic acid were added. Finally, 6 mL of water was added after another 5 min. The solution was stirred during the whole process and for 1 day after the addition of water. It was then dried under vacuum at room temperature.

$CaZr_{0.5}Ti_{0.5}O_3$, $CaZrO_3$, and $CaTiO_3$ samples were prepared by the reaction of predried $CaCO_3$, TiO_2, and ZrO_2. All the powders were mixed and ground thoroughly prior to heating at 1400 °C for 5 h. The products were identified by powder diffraction before further grinding and heating (1500 °C, 10 h).

Powder X-ray Diffraction. All data were collected using Cu Kα radiation on a Scintag X1 diffractometer equipped with a Scintag Peltier cooled solid-state detector. Diffraction patterns were recorded (20°−70° 2θ, 2.5°/min) for each of the samples. Additionally, data for Rietveld analysis were acquired for $Ca(Zr_xTi_{1-x})O_3$ (x = 0, 0.25, 0.5, 0.75, 1) samples (C1, C2, H3, H6, and H9, see Table 1) over the range 5°−135° 2θ in steps of 0.02° using a counting time of 10 s per step.

Rietveld Analyses. Refinements were performed for phase pure perovskite $Ca(Zr_xTi_{1-x})O_3$ (x = 0, 0.25, 0.5, 0.75, 1) samples. The profile parameters, lattice constants, background parameters, and scale factors were varied along with the atomic position and displacement parameters. Rietveld analyses were also performed for many of the other samples using

(15) Penner-Hahn, J. E. *Coord. Chem. Rev.* **1999**, *190−192*, 1101−1123.
(16) Koningsberger, D. C.; Prins, P. *X-ray Absorption: Principles, Applications, Techniques of EXAFS, SEXAFS and XANES*; Wiley: New York, 1988.
(17) Perel, J.; Deslattes, R. D. *Phys. Rev. B* **1970**, *2*, 1317−1323.
(18) Hanajiri, Y.; Matsui, T.; Arita, Y.; Nagasaki, T.; Shigematsu, H.; Harami, T. *Solid State Ionics* **1998**, *108*, 343−348.
(19) Farges, F.; Ewing, R. C.; Brown, G. B. *J. Mater. Res.* **1993**, *8*, 1983−1995.
(20) Kolb, U.; Gutwerk, D.; Beudert, R.; Bertagnolli, H. *J. Non-Cryst. Solids* **1997**, *217*, 162−166.
(21) Peter, D.; Ertel, T. S.; Bertagnolli, H. *J. Sol-Gel Sci. Technol.* **1995**, *5*, 5−14.
(22) Ahlfanger, R.; Bertagnolli, H.; Ertel, T.; Kolb, U.; Peter, D.; Nass, R.; Schmidt, H. *Ber. Bunsen-Ges. Phys. Chem.* **1991**, *95*, 1286−1289.
(23) Kolb, U.; Abraham, I.; Gutwerk, D.; Ertel, T. S.; Horner, W.; Bertagnolli, H.; Merklein, S.; Sporn, D. *Physica B* **1995**, *208/209*, 601−603.
(24) Kolb, U.; Gutwaerk, D.; Beudert, R.; Ertel, T. S.; Abraham, I.; Horner, W.; Bertagnolli, H. *EXAFS: Structure Investigations on PZT Precursors*; Daresbury Laboratory: UK, 1995.
(25) Antonioli, G.; Bersani, D.; Lottici, P. P.; Manzini, I.; Bassi, S.; Gnappi, G.; Montenero, A. *J. Phys. IV (Paris)* **1997**, *7*, C2−1161.
(26) Malic, B.; Arcon, I.; Kosec, M.; Kodre, A. *J. Sol-Gel Sci. Technol.* **1997**, *8*, 343−346.
(27) Sengupta, S. S.; Ma, L.; Adler, D. L.; Payne, D. A. *J. Mater. Res.* **1995**, *10*, 1345−1348.
(28) Malic, B.; Arcon, I.; Kosec, M.; Kodre, A. *J. Mater. Res.* **1997**, *12*, 2602−2611.
(29) Ravel, B.; Stern, E. A. *J. Phys. IV* **1997**, *7*, C2 1223−1224.
(30) Sicron, X.; Yacoby, Y.; Stern, E. A.; Dogan *J. Phys. IV* **1997**, *7*, C2 1047−1049.
(31) Ravel, B.; Stern, E. A. *Phys. B* **1995**, *208/209*, 316−318.
(32) Sicron, N.; Ravel, B.; Yacoby, Y.; Stern, E. A.; Dogan, F.; Rehr, J. J. *Phys. B* **1995**, *208/209*, 319−320.

Table 1. Samples Examined and the Δk ($Å^{-1}$) Available for EXAFS Analysis

sample code	sample	synthesis procedure[a]	Ti K-edge Δk ($Å^{-1}$)	Zr K-edge Δk ($Å^{-1}$)
C1	$CaZrO_3$	mixed oxide 1200 °C	N/A	1−19.93
C2	$CaTiO_3$	mixed oxide 1200 °C	1−15.33	N/A
C3	$Ca(Zr_{0.5}Ti_{0.5})O_3$	mixed oxide 1500 °C	N/A	0.43−19.93
H1	$Ca(Zr_{0.5}Ti_{0.5})O_3$	HSG xerogel	1−13.50	1−16.20
H2	$Ca(Zr_{0.5}Ti_{0.5})O_3$	HSG 500 °C	1−13.00	1−15.40
H3	$Ca(Zr_{0.5}Ti_{0.5})O_3$	Homo SG 1200 °C	1−13.50	1−16.60
IH1	$Ca(Zr_{0.5}Ti_{0.5})O_3$	IHSG xerogel	N/A	1−16.73
IH2	$Ca(Zr_{0.5}Ti_{0.5})O_3$	IHSG 500 °C	N/A	1−16.00
IH3	$Ca(Zr_{0.5}Ti_{0.5})O_3$	IHSG 1200 °C	N/A	1−16.90
A1	$Ca(Zr_{0.5}Ti_{0.5})O_3$	AAM xerogel	N/A	1−17.90
A2	$Ca(Zr_{0.5}Ti_{0.5})O_3$	AAM 500 °C	N/A	1−18.00
A3	$Ca(Zr_{0.5}Ti_{0.5})O_3$	AAM 1200 °C	N/A	1−16.70
H4	$Ca(Zr_{0.25}Ti_{0.75})O_3$	HSG xerogel	N/A	N/A
H5	$Ca(Zr_{0.25}Ti_{0.75})O_3$	HSG 500 °C	N/A	N/A
H6	$Ca(Zr_{0.25}Ti_{0.75})O_3$	HSG 1200 °C	1−13.50	1−15.92
H7	$Ca(Zr_{0.75}Ti_{0.25})O_3$	HSG DG	N/A	N/A
H8	$Ca(Zr_{0.75}Ti_{0.25})O_3$	HSG 500 °C	N/A	N/A
H9	$Ca(Zr_{0.75}Ti_{0.25})O_3$	HSG 1200 °C	1−15.00	1−16.52
H10	$CaZrO_3$	HSG xerogel	N/A	1−17.30
Z1	ZrO_2	commercial monoclinic	N/A	1−16.61

[a] HSG = homogeneous sol−gel; IHSG = inhomogeneous sol−gel; AAM = acetic acid modified method; N/A = not applicable.

a limited data set (20°−70° 2θ) to obtain estimates of the lattice constants for the sample's perovskite component.

ICP-AES Analyses. All the high-temperature CZT, CZ, and CT samples were fused in molten lithium tetraborate at 1050 °C for 30 min and the resulting glass was dissolved in 4% HNO_3 (v/v). Analyses were performed using a Perkin-Elmer Optima 3000 instrument. The Zr:Ti mole ratios were all within 3% of the expected values, and the calcium/transition metal mole ratios were typically within 4% of the expected value, although sample IH3 was estimated to have 6% excess calcium.

Thermal Analyses. A Seiko DTA/TGA 320 system was used for each of the xerogel samples over the range 30°−1000 °C using a ramp of 20 °C/min and air flowing at 200 mL/min.

XAS Data Collection. Zr and Ti K-edge transmission X-ray absorption spectra (XAS) were measured using beam line X11A at the NSLS, Brookhaven. A Si(111) double-crystal monochromator was employed along with a 10×1 mm^2 beam. Spectra were obtained using three ion chambers with the sample between the first two and a reference foil between the second and third. Twenty percent and sixty percent I_0 harmonic rejection were used for the Zr and Ti K-edge spectra, respectively. Three scans were acquired for each sample and averaged prior to analysis. A summary of the data collected and the naming scheme for the samples are presented in Table 1.

XAS Data Analyses. All the analyses were performed using EXAFSPAK.[33] Phase and amplitude functions were calculated using FEFF7.[34]

Pre-edge peak heights and positions were obtained from the Ti XANES spectra. The data were normalized and a second derivative was calculated to find the peaks. These positions were used in fitting the normalized spectra. A combination of pseudo-Voigt functions for the pre-edge features and a step function to model the edge were employed. The extracted peak positions and heights along with a plot showing the fits are available as Supporting Information.

Quantitative analyses of the both the Zr and Ti K-edge EXAFS data were only performed for the oxygen shells. The data for $CaZrO_3$ and $CaTiO_3$ were fitted to extract E_0 values that could be used in the other analyses. Structural models were obtained from the work of Koopmans et al.[35] The crystal structures of $CaZrO_3$ and $CaTiO_3$ have three symmetry inequivalent M−O distances (M = Zr or Ti). Two models were employed in fitting the Zr−O EXAFS data; one oxygen subshell with 6 coordination and three oxygen subshells with 2 + 2 + 2 coordination. The fitting results are shown in Table 2. Two models were also employed in fitting all of the Ti−O EXAFS; one oxygen subshell with 6 coordination and two oxygen subshells with 4 + 2 coordination. The 4 + 2 model was adopted rather than a 2 + 2 + 2 model as four of the Ti−O distances in $CaTiO_3$ are very close to one another. As the XANES data indicated that samples H1 and H2 might contain 5-coordinated titanium, a model based on the structure of Na_2TiSiO_5[36] was also explored (4 + 1 coordination) for these samples. The fitting results are presented in Table 3.

Table 2. Parameters from Fitting the Zr−O EXAFS Data (The Mean Zr−O Distance Obtained Using a Three-Shell Model Is Compared with the Value from a One-Shell Model)

	three-shell			one-shell		
sample	R_{Zr-O} (Å)	σ^2 ($Å^2$)	N^a	R_{Zr-O} (Å)	σ^2 ($Å^2$)	N^a
H1	2.125	0.0044	6	2.105	0.0090	6
H2	2.119	0.0057	6	2.105	0.0096	6
H3	2.087	0.0026	6	2.079	0.0041	6
IH1	2.111	0.0053	6	2.100	0.0087	6
IH2	2.119	0.0045	6	2.107	0.0091	6
IH3	2.094	0.0038	6	2.094	0.0039	6
A1	2.177	0.0010	6	2.170	0.0072	6
A2	2.147	0.0014	6	2.123	0.0104	6
A3	2.083	0.0038	6	2.081	0.0045	6
H6	2.078	0.0015	6	2.069	0.0041	6
C3	2.090	0.0038	6	2.077	0.0047	6
H9	2.091	0.0012	6	2.084	0.0041	6

[a] N, number of oxygen atoms at this distance.

Results and Discussion

Crystallization Studies. Powder XRD data for CZT samples heat-treated in the range 200−1200 °C are available as Supporting Information. Essentially phase-pure perovskites were obtained at 1200 °C for all the compositions prepared by the HSG and AAM methods. However, a two-phase perovskite mixture was observed for our CZT 50/50 samples prepared by either the direct reaction of oxides or the inhomogeneous sol−gel method. Previous work on the phase relations in the ternary

(33) George, G. N.; Pickering, I. J. *EXAFSPAK A Suite of Programs for Analysis of X-ray Absorption Spectra*.

(34) Zabinsky, S. I.; Rehr, J. J.; Ankubinov, A.; Albers, R. C.; Eller, M. J. *Phys. Rev. B* **1995**, *52*, 2995.

(35) Koopmans, H. J. A.; Van de Velde, G. M. H.; Gellings, P. J. *Acta Crystallogr.* **1983**, *C39*, 1323−1325.

(36) Nyman, H.; O'Keeffe, M. *Acta Crystallogr.* **1978**, *B34*, 905−906.

Table 3. Best Fit Parameters for the Ti−O EXAFS (The Average Ti−O Distance Obtained from a Two-Shell Fit is Compared to the Value Resulting from a One-Shell Fit)

	two-shell			one-shell		
sample	R_{Ti-O} (Å)	σ^2 (Å^2)	N^a	R_{Ti-O} (Å)	σ^2 (Å^2)	N^a
C2	1.927	0.0039	4	1.950	0.0051	6
	1.986	0.0044	2			
H3	1.933	0.0019	4	1.962	0.0056	6
	2.050	0.0019	2			
H2	1.753	0.0057	1	NA[b]	NA[b]	NA[b]
	1.930	0.0064	4			
H1	1.758	0.0046	1	NA[b]	NA[b]	NA[b]
	1.932	0.0056	4			
H7	1.941	0.0022	4	1.972	0.0065	6
	2.068	0.0020	2			
H6	1.931	0.0021	4	1.958	0.0051	6
	2.035	0.0024	2			

[a] *N*, number of oxygen atoms at this distance. [b] NA, no values are given as the fit quality was very poor.

system $CaO-ZrO_2-TiO_2$ at 1200,[4] 1300,[37] and 1450−1550 °C[38] showed that a mixture of perovskites was obtained upon firing $Ca(Zr_xTi_{1-x})O_3$ samples (two phase for $0.22 < x < 0.78$ at 1200 °C[4]) at temperatures below 1450−1550 °C. This was attributed to difficulties in reaching equilibrium.[4] The preparation of single-phase perovskite at 1200 °C via the homogeneous sol−gel and AAM routes clearly illustrates one of the advantages that wet chemical methods can offer over direct reaction of mixed oxides.

None of our samples crystallized in a straightforward fashion. Many of them contained a perovskite upon drying at 200 °C. However, at low temperatures, there was often evidence for the presence of $CaCO_3$ and at intermediate temperatures CaO was formed before the calcium-rich component completely disappeared. There was also evidence for the presence of a fluorite-related material in many of the samples subjected to low or intermediate temperature heat treatments.

Formation of Perovskite at Low Temperature. The $CaTiO_3$, $Ca(Zr_{0.25}Ti_{0.75})O_3$, and $Ca(Zr_{0.5}Ti_{0.5})O_3$ xerogels prepared using the HSG method and the $Ca(Zr_{0.5}Ti_{0.5})O_3$ xerogel prepared by the IHSG route contained perovksite. However, the $CaZrO_3$ and $Ca(Zr_{0.75}Ti_{0.25})O_3$ xerogels prepared by the HSG route and the $Ca(Zr_{0.5}Ti_{0.5})O_3$ xerogel prepared by the AAM route did not. Remarkably, the $Ca(Zr_{0.5}Ti_{0.5})O_3$ xerogel prepared by the IHSG route contained two distinct perovskites, identified as almost pure $CaTiO_3$ and $CaZrO_3$. Clearly, the presence of crystalline perovskite in the dry gels depends both upon the processing chemistry employed and the zirconium content of the solid solution. No perovskite was observed at low temperature for the AAM-processed sample and for the homogeneous alkoxide sol−gel samples the amount of crystalline perovskite increased as the titanium content increased. As the zirconium-rich samples prepared by the homogeneous sol−gel method do not contain any perovskite at low temperature, it is tempting to attribute the appearance of perovskite CZ in the inhomogeneous CZT 50/50 sample to a seeding effect. Part of the titanium-rich component in the sample crystallizes at low temperatures and seeds the growth of perovskite CZ.

It has previously been observed that the formation of perovskite at low temperatures can depend on the precursors that are used, presumably because they influence the hydrolysis and polycondensation reactions that take place. For example, it is known that $BaTiO_3$ dry gels prepared from titanium alkoxides contain crystalline perovskite when barium ethoxide is used instead of barium acetate.[39] A dependence of the perovskite crystallization temperature on solid-solution composition has also been observed in the PZT system.[40] In our previous work on PZT, no perovskite was present in the dry gel and the trend in crystallization temperatures was related to the melting points of the different compositions.[40]

Calcium-Rich Phase at Low to Intermediate Temperatures. Many of the samples contained $CaCO_3$ after low-temperature heat treatment and CaO after heating to higher temperatures. For example, for the $Ca(Zr_{0.5}Ti_{0.5})O_3$ prepared by the HSG method, perovskite, $CaCO_3$, and an amorphous component coexisted in the xerogel. After a 600 °C heat treatment there was no $CaCO_3$ present, but there was evidence for CaO along with a fluorite-like phase and perovskite. Higher temperature treatment (1200 °C, 20 h) led to the disappearance of both the fluorite-like phase and the CaO and to the formation of pure perovskite. Similar behavior was observed for the $CaTiO_3$, $Ca(Zr_{0.25}Ti_{0.75})O_3$, $Ca(Zr_{0.75}Ti_{0.25})O_3$, and $CaZrO_3$ gels.

The failure of all the CZT preparation routes to produce compositionally homogeneous materials and in particular the presence of a calcium-rich phase in many cases is not surprising. Calcium is unlikely to be uniformly incorporated into the backbone of the polymer network formed by hydrolysis of the metal alkoxide solution, as its chemistry is very different from that of the other metal ions. Previous workers have also observed compositional inhomogenieties in sol−gel syntheses of related materials. For example, PbO is often observed at low temperature during the preparation of PZT via solution methods,[41−43] and a sol−gel preparation of $Mg_{0.95}Ca_{0.05}TiO_3$,[10] using titanium isopropoxide and alkaline metal nitrates precursors, produced crystalline metal nitrates in samples that had been heated to 300 °C. In our work, it seems likely that a distinct calcium-rich phase is formed by the decomposition of the nitrate to calcium oxide and then at low temperatures the oxide reacts with the decomposition products from the residual organics to form a carbonate. The formation of carbonates is quite common during sol−gel syntheses.[13,44]

Fluorite-Like Phase. Upon heating of the dry gels, more than one transition-metal-containing phase crys-

(37) Figueiredo, M. O.; Correia Dos Santos, A. In *Zirconia 88: Advances in Zirconia Science and Technology*; Meriani, S., Palmonari, C., Eds.; Elsevier Science: New York, 1988; pp 81−87.
(38) Coughanour, L. W.; Roth, R. S.; Marzullo, S.; Sennett, F. E. *J. Res. Nat. Bur. Stand.* **1955**, *54*, 195.
(39) Mazdiyasni, K. S.; Dollof, R. T.; Smith, J. S. *J. Am. Ceram. Soc.* **1969**, *52*, 523−526.
(40) Wilkinson, A. P.; Speck, J. S.; Cheetham, A. K.; Natarajan, S.; Thomas, J. M. *Chem. Mater.* **1994**, *6*, 750−754.
(41) Ahmad, A.; Bedard, P.; Wheat, T. A.; Kuriakose, A. K.; McDonald, A. G. *J. Solid State Chem.* **1991**, *93*, 220−227.
(42) Lin, C. T.; Scanlan, B. W.; McNeill, J. D.; Webb, J. S.; Li, L.; Lipeles, R. A.; Adams, P. M.; Leung, M. S. *J. Mater. Res.* **1992**, *7*, 2546−2554.
(43) Faure, S. P.; Barboux, P.; Gaucher, P.; Livage, J. *J. Mater. Chem.* **1992**, *2*, 713−717.
(44) Samuneva, B.; Jambazov, S.; Lepkova, D.; Dimitriev, Y. *Ceram. Int.* **1990**, *16*, 355−360.

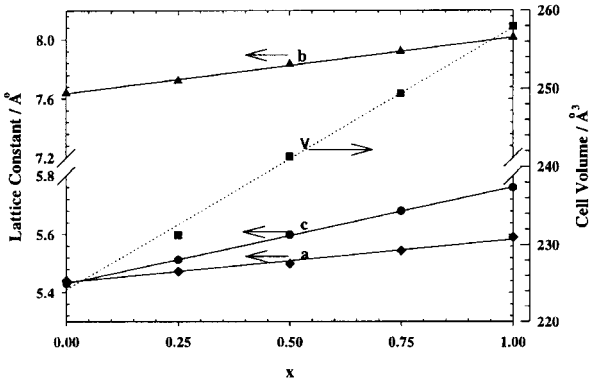

Figure 1. Variation of the lattice constants and unit cell volume with composition for the perovskite $CaZr_xTi_{1-x}O_3$ solid solution. The values were obtained from a Rietevld analysis of the diffraction data for samples C1, C2, H3, H6, and H9.

tallized. Even at low temperatures (≈500 °C) a fluorite-like phase was present in nearly all of the samples. It increased in crystallinity, as evidenced by a sharpening of its Bragg peaks, at higher temperatures and eventually disappeared upon heating to 1200 °C for long periods of time.

Calcium-stabilized zirconia and several well-known materials with composition $Ca_{0.20}Zr_{0.80-x}Ti_xO_y$ (x = 0.04−0.25) have fluorite-related structures.[45,46] The maximum solubility of CaO and TiO_2 in a c-ZrO_2 matrix has been reported to be 17% and 10%, respectively.[2] If these solubility data are applicable to materials prepared via sol−gel methods, the fluorite-related phase must be both calcium- and titanium-deficient when compared to the bulk sample composition. While there is clearly a calcium-rich phase present at low temperatures, there is no diffraction evidence for a titanium-rich phase. This suggests that either the titanium is present as an amorphous/nanocrystalline component or the titanium content of the fluorite-like phase is much higher than that indicated by the published solubility data. There have been several reports of metastable titanium-containing fluorites formed during the synthesis of PZT.[40,47−49]

A titanium deficiency in the fluorite-like phase should influence the crystallization of perovskite CZT. For example, if perovskite is formed from a titanium-deficient fluorite, then the perovskite that crystallizes at low temperatures will also be titanium-deficient. As the lattice constants of perovskite CZT vary with composition (see Figure 1), we determined them for the perovskite component that was present in a series of mixed-phase materials that had been heat-treated at different temperatures (values available as Supporting Information) and then compared them with those that we obtained for phase pure perovksites with different compositions. The observed lattice constants for the multiphase samples were independent of the heat treatment conditions used and in good agreement with those found for phase pure perovskite with the same bulk compositions as the samples examined (samples C1, C2, H3, H6, and H9). This clearly indicates that the initially formed perovskite has the same composition as the bulk sample and implies that the fluorite-like phase has the same zirconium-to-titanium ratio as the bulk sample.

Inhomogeneous Sol−Gel Samples. Both the dry gel and fully crystallized CZT 50:50 samples prepared by the IHSG route contained two distinct perovksites. Their compositions were established from their lattice constants (a = 5.596, b = 8.008, c = 5.744 Å and a = 5.383, b = 7.641, c = 5.438 Å, respectively). The fully crystallized sample was found to be essentially a physical mixture of $CaZrO_3$ and $CaTiO_3$.

This observation has implications for the nature of the gels formed by the hydrolysis of the metal alkoxides. In a previous study of PZT 50/50,[50] we prepared a sample by a similar IHSG procedure, but only a short hydrolysis time was employed prior to mixing the PZ and PT sols. The sols were both of low viscosity. The resulting PZT 50/50 sample's compositional inhomogeneity was not readily distinguishable from that of a sample heated under similar conditions but prepared by the conventional hydrolysis of mixed PZ and PT precursors. We concluded from this observation that either (i) the zirconium- and titanium-rich polymers (sols) reacted with one another to form a gel (polymer) with a more homogeneous distribution of zirconium and titanium in it or (ii) the conventional hydrolysis approach produced gels with an inhomogeneous distribution of zirconium and titanium. On the basis of our observations in the CZT system, mixed prehydrolyzed CZ and CT precursors (zirconium- and titanium-rich sols) apparently do not readily undergo exchange reactions with one another to produce compositionally homogeneous polymers. We dried our mixture of CZ and CT sols at 200 °C in a vacuum oven. Removal of the solvent took several hours, but there is no evidence for any compositional homogenization during drying. The origin of the differences between the CZT and PZT systems is still not entirely clear, but it is probably in part due to the different hydrolysis procedures that were used.

TGA Studies. Plots of the TGA data obtained upon heating the CZT dry gels in air are available as Supporting Information. With the exception of the materials made by the AAM route, all of the samples showed similar behavior. There were losses at <150, 150−450, 450−550, and >650 °C. The $Ca(Zr_{0.75}Ti_{0.25})O_3$ and $Ca(Zr_{0.5}Ti_{0.5})O_3$ made by IHSG route and the $CaZrO_3$ samples showed an extra weight loss at ≈750 °C. It is notable that all of these materials have a zirconium-rich component in their gels. The total weight loss amounted to 12−27% for the five samples made by alkoxide sol−gel methods. It is likely that the weight loss at <150 °C results from the evaporation of alcohol and water. The burnout of organics presumably occurs in the 150−450 °C range. At higher temperatures (>650 °C and at ≈750 °C) the weight losses may be due to the removal of residual carbon-rich material (coke) or organics[11] and the decomposition of carbonates. The

(45) Kashaev, A. A.; Ushchapovskaya, Z. F. *Kristallografiya* **1969**, *14*, 1064−165.
(46) Lin, J. S.; Shen, P. *J. Solid State Chem.* **1996**, *126*, 177−183.
(47) Kwok, C. K.; Desu, S. B. *Appl. Phys. Lett.* **1992**, *60*, 1430−1432.
(48) Seifert, A.; Lange, F. F.; Speck, J. S. *J. Mater. Res.* **1995**, *10*, 680−691.
(49) Polli, A. D.; Lange, F. F.; Levi, C. G. *J. Am. Ceram. Soc.* **2000**, *83*, 873−881.
(50) Wilkinson, A. P.; Xu, J.; Pattanaik, S.; Billinge, S. J. L. *Chem. Mater.* **1998**, *10*, 3611−3619.

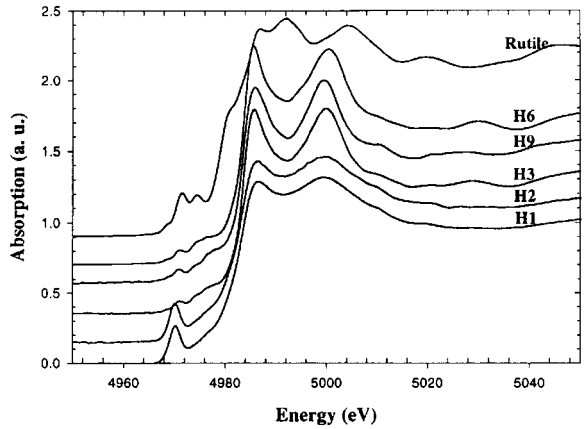

Figure 2. Ti K-edge XANES spectra for a series of CZT 50/50 samples, prepared using alkoxide sol−gel chemistry, that have been heated to 200, 500, and 1200 °C (H1, H2, and H3, respectively), along with spectra for rutile and perovskite CZT 75/25 (H9) and 25/75 (H6).

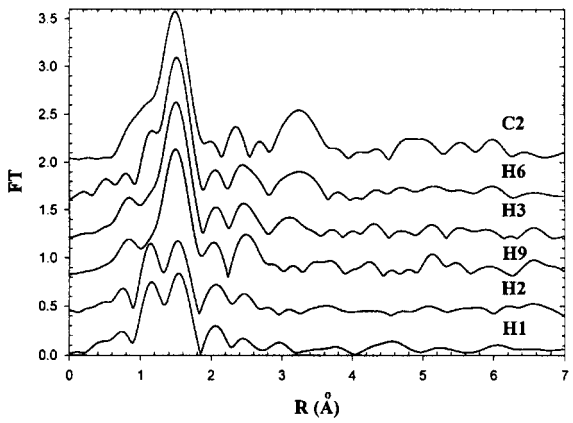

Figure 3. Fourier-transformed Ti K-edge EXAFS for perovskite CZT samples with compositions 0/100, 25/75, 50/50, and 75/25 (samples C2, H6, H3, and H9) and CZT 50/50 samples that had been heated to 200 and 500 °C (H1 and H2). The peak at around 3.4 Å is very sensitive to the bulk composition of the samples.

samples heated for 5 h in air only contained calcium carbonate at 500 °C and below, and bulk calcium carbonate loses weight above 600 °C under the conditions used for the TGA experiments.

The AAM material gave a TGA curve that was very different from those of the alkoxide sol−gel samples. It had three significant weight losses with onsets at ≈60, ≈200, and ≈600 °C. They can probably be attributed to the loss of physisorbed moisture, organic burnout, and the decomposition of $CaCO_3$, respectively. The total weight loss for this sample was ≈55%, which is much greater than that for the alkoxide sol−gel samples and may be related to the drying procedure that was used for this material.

X-ray Absorption Studies. Ti K-edge X-ray absorption near-edge structure (XANES) spectra for all the samples are shown in Figure 2. They can be split into two groups on the basis of the observed pre-edge features: one with three peaks of low intensity and the other with a single intense peak.

The observation of two types of pre-edge features strongly suggests that there is a change in the coordination environment for titanium in some of the CZT samples as the materials are heat-treated. Strong pre-edge features, such as those observed for samples H1 and H2, are commonly attributed to transitions that are only allowed when the metal is in a noncentrosymmetric environment. Weaker features are found for titanium in approximately centrosymmetric environments.[51,52] The heights and positions of the pre-edge peaks for samples H1 and H2 can be related to the geometry of the Ti−O coordination polyhedron. Pre-edge peaks have the greatest height for ^{4}Ti (^{4}Ti, ^{5}Ti, and ^{6}Ti represent 4-, 5-, and 6-coordinated titanium), and the major feature found in spectra of ^{6}Ti is shifted to higher energy by 2 ± 0.2 eV when compared with that observed for ^{4}Ti.[11,53−60] The energies and heights of the pre-edge features for ^{5}Ti fall between the values observed for ^{4}Ti and ^{6}Ti. The pre-edge peaks for our samples H1 and H2 are shifted to lower energy by 0.8 eV when compared to those for perovskite CZT (samples H3, H6, and H9), suggesting that most of the Ti in the former samples may be five-coordinated.

Zr K-edge XANES spectra for both the crystalline and amorphous CZT samples are available as Supporting Information. The broad largely featureless absorption jump provides little information. However, the spectrum for sample A1 is different from that observed for all of the other amorphous samples, suggesting that it had a distinct zirconium environment.

Ti EXAFS. The Ti K-edge FTs are shown in Figure 3. The structural similarity of the two CZT 50/50 samples that had been heated at low temperature (H1 and H2) is confirmed by inspection of their FTs. A split peak is observed for both samples at distances consistent with oxygen backscattering and there are no metal−metal peaks above the noise level. All the FTs of the crystalline CZT samples (C2, H3, H6, and H9) show one strong peak at ≈1.6 Å due to backscattering from oxygen. The peak at 3.4 Å in the FTs for the crystalline CZT samples is due to backscattering from Ti/Zr. Its height increases along with the Ti content of the solid solution.

Good fits to the Ti−O EXAFS data for samples H1 and H2 were obtained when a two subshell model was used with one oxygen at 1.75 Å and four at 1.93 Å. The average Ti−O distance for both of the samples (1.89 ± 0.01 Å) is consistent with the value found for five-coordinated titanium (1.90 ± 0.01 Å) by Zechmann et al.[61] in a Ti/Zr mixed metal−alkoxide. The observed

(51) Vedrinskii, R. V.; Kraizman, V. L.; Novakovich, A. A.; Demekhin, P. V.; Urazhdin, S. V. *J. Phys. Condens. Matter* **1998**, *10*, 9561−9580.
(52) Vedrinskii, R. V.; Kraizman, V. L.; Novakovich, A. A.; Demekhin, P. V.; Urazhdin, S. V.; Ravel, B.; Stern, E. A. *J. Phys. IV (Paris)* **1997**, *7*.
(53) Farges, F. *J. Non-Cryst. Solids* **1996**, *204*, 53−64.
(54) Farges, F.; Brown, G. B.; Rehr, J. J. *Geochim. Cosmochim. Acta* **1996**, *60*, 3023−3038.
(55) Farges, F.; Brown, G. E.; Navrotsky, A.; Gan, H.; Rehr, J. J. *Geochim. Cosmochim. Acta* **1996**, *60*, 3039−3053.
(56) Farges, F.; Brown, G. E.; Rehr, J. J. *Phys. Rev. B* **1997**, *56*, 1809−1819.
(57) Farges, F. *Am. Mineral.* **1997**, *82*, 36−43.
(58) Farges, F. *Am. Mineral.* **1997**, *82*, 44−50.
(59) Farges, F.; Brown, G. B. *Geochim. Cosmochim. Acta* **1997**, *61*, 1863−1870.
(60) Farges, F.; Brown, G. B.; Rehr, J. J. *J. Phys. IV (Paris)* **1997**, *7*, C2 191−193.
(61) Zechmann, C. A.; Huffman, J. C.; Folting, K.; Caulton, K. G. *Inorg. Chem.* **1998**, *37*, 5856−5861.

distances are also in good agreement with those found for many titanium silicate compounds that typically contain Ti in a square pyramidal environment with one short Ti=O distance (1.69−1.78 Å) and four longer Ti−O bonds (1.9−2.0 Å).[58] Similar EXAFS results have been reported by Kodre et al. for amorphous PT and PZT samples prepared by a sol−gel method.[26] They proposed that Ti was coordinated by oxygen at 1.73 and 1.90 Å. The occurrence of five-coordinated titanium in the low-temperature materials prepared by the HSG route may be due to the steric difficulty of accommodating six ligands around the rather small Ti(IV) ion.

For the samples heated to higher temperatures, a two subshell model with four oxygen atoms at a shorter distance and two at a longer distance gave a better fit to the data than a five-coordinated model. The average Ti−O distance for all of the perovskite samples was between 1.95 and 1.97 Å (see Table 3) and it only varied slightly with solid-solution composition.

Zr EXAFS. The Fourier transform magnitudes (FTs) for our Zr K-edge EXAFS data on the CZT 50/50 samples are grouped by sample preparation method in Figure 4, parts a, b, and c (HSG, IHSG, and AAM, respectively). The FTs for nearly all of the low-temperature samples (H1, H2, IH1, and IH2) are similar to one another with only one well-defined peak at ≈1.7 Å that can be attributed to oxygen backscattering. Additional well-defined peaks in the FTs are observed for the samples treated at higher temperature (H3, IH3, and A3). The largest peak is still found at ≈1.7 Å. However, an additional peak at ≈3.6 Å is due to backscattering from nearest neighbor transition metals. It is notable that the FT for the dry CZT gel prepared by the AAM route (sample A1) is different from that of the other materials prepared at low temperature as a peak is present at ≈3.2 Å. After the samples are heated to 500 °C, all the FTs are similar to one another.

Compositional Homogeneity of the Dry Gel Prepared by the AAM Route. A comparison was made between the FTs of the data for sample A1 and monoclinic ZrO_2 (available as Supporting Information). The position of the second peak in the FT for sample A1 is very close to the Zr−Zr peak in the FT of monoclinic ZrO_2, although the peak amplitude is quite different. This similarity suggested a contribution from zirconium to the second peak in A1's FT. To better establish what element(s) contribute(s) to this peak, it was back-transformed into *k* space. The Zr−Zr peak for monoclinic ZrO_2 was also back-transformed. The expected EXAFS signal for a Zr−Ti peak arising from metals separated by the metal−metal distance found in monoclinic ZrO_2 was calculated using FEFF7. A comparison of the signal from the unknown peak with the Zr−Zr EXAFS for monoclinic ZrO_2 and the theoretical Zr−Ti EXAFS was made (available as Supporting Information). The maximum in the amplitude envelope (k_{max}) for the Zr−Zr EXAFS from ZrO_2 occurs at ≈10.5 $Å^{-1}$ and is in good agreement with that for sample A1 (≈10 $Å^{-1}$) while that for the Ti backscatter occurred at ≈7.5 $Å^{-1}$. This suggests a dominant contribution from zirconium to the backscattering, but the presence of a significant number of Zr−Ti pairs cannot be excluded. Interestingly, Payne and other workers have reported that alkoxide-processed PZT gels contain predominantly Zr−O−Zr and Ti−O−Ti links and very few Zr−O−Ti links on the basis of an EXAFS analysis.[27,62]

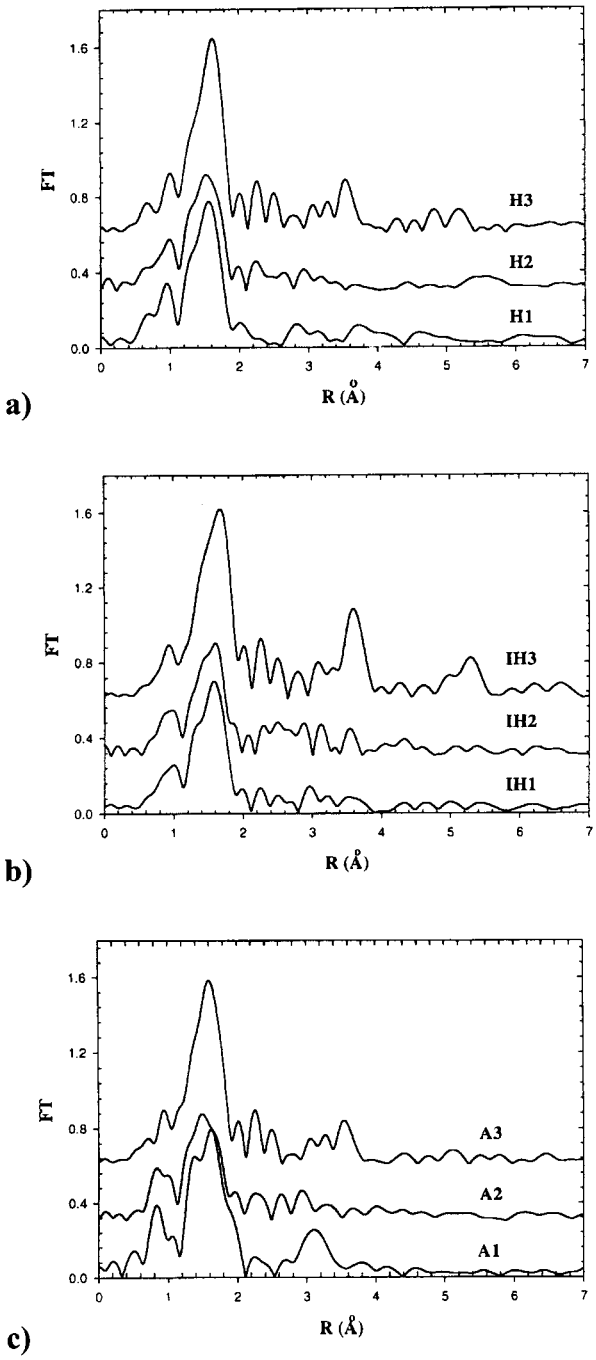

Figure 4. Fourier-transformed Zr K-edge EXAFS for $Ca(Zr_{0.5}Ti_{0.5})O_3$ prepared by (a) the homogeneous sol−gel method and heated to 200, 500, and 1200 °C (H1, H2, and H3, respectively), (b) the inhomogeneous sol−gel method and heated to 200, 500, and 1200 °C (IH1, IH2, and IH3), and (c) the acetic acid method and heated to 200, 500, and 1200 °C (A1, A2, and A3).

Sensitivity of Zr EXAFS to CZT Solid-Solution Composition. The Zr K-edge FTs for samples H6, H3, H9, and C1 are shown in Figure 5. As the Zr content increases from 0.25 to 1, the intensity of the peak at ≈3.6 Å increases and it also shifts to slightly lower distances. Clearly, this peak is very sensitive to the Zr content of perovskite CZT. For the samples studied, the

(62) Arcon, I.; Malic, B.; Kodre, A.; Kosec, M. *J. Synchrotron Rad.* **1999**, *6*, 535−536.

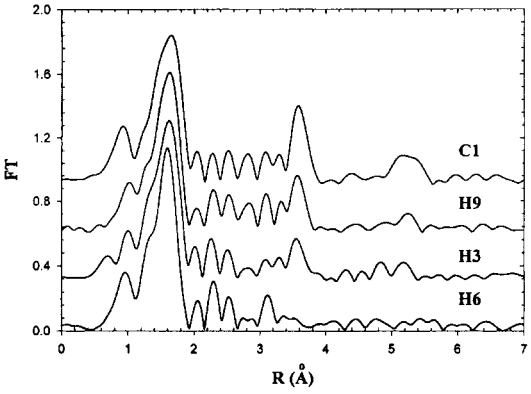

Figure 5. Fourier-transformed Zr K-edge EXAFS for perovskite CZT samples with compositions 100/0, 75/25, 50/50, and 25/75 (C1, H9, H3, and H6). The peak at around 3.6 Å is very sensitive to the bulk compositions of the samples.

peak height is linearly related to the zirconium concentration. However, simulations indicate that the peak at ≈3.6 Å in the FT depends on the assumed Zr−Zr and Zr−Ti distances as well as the amount of Zr and Ti around each absorber.

Compositional Homogeneity of the Sol−Gel-Processed Solid Solutions. Although the EXAFS are very sensitive to local composition, a quantitative analysis to determine on average how many Zr and Ti there are around an absorber is very difficult. Consequently, we chose to test the compositional homogeneity of our solid-solution samples by comparing some of the spectra with weighted averages of other spectra.

The observed EXAFS spectrum for zirconium in CZT is a sum of the contributions from each of the backscattering atoms. If the geometries of the Zr−O−Zr and Zr−O−Ti links that occur are independent of solid-solution composition, it should be possible to reproduce a spectrum for say CZT 50/50 by summing together the spectra of two other samples with different compositions. The only requirement is that the average number of Zr−O−Zr links around zirconium is the same in both the CZT 50/50 sample and the hypothetical mixture. If all the samples used in the comparison were random solid solutions and a spectrum was measured for a physical mixture of CZT 25/75 and CZT 75/25, then a 75/25 mix of the samples would on average have the same number of Zr−O−Zr links around each zirconium as a single-phase CZT 50/50 sample. However, spectra for the CZT 25/75 (on average 1.5Zr + 4.5Ti around each absorber) and CZT 75/25 (on average 4.5Zr + 1.5Ti around each absorber) samples were measured separately and the EXAFS normalized by the edge jump, so a 50/50 mixture of the two spectra should closely resemble that for a CZT 50/50 sample (on average 3Zr + 3Ti around each absorber) if all the specimens were random solid solutions.

We performed two comparisons to learn about the homogeneity of our HSG samples. The Zr K-edge data for CZT 50/50 (H3) are compared with a 50% + 50% sum of CZT 25/75 (H6) and CZT 75/25 (H9) spectra in Figure 6a. The FT magnitudes of both sets of EXAFS are shown in Figure 6b. The agreement between the FT of the average and the FT for the CZT 50/50 sample is moderate in the region corresponding to Zr−O−Zr and Zr−O−Ti backscattering. This may indicate that one or

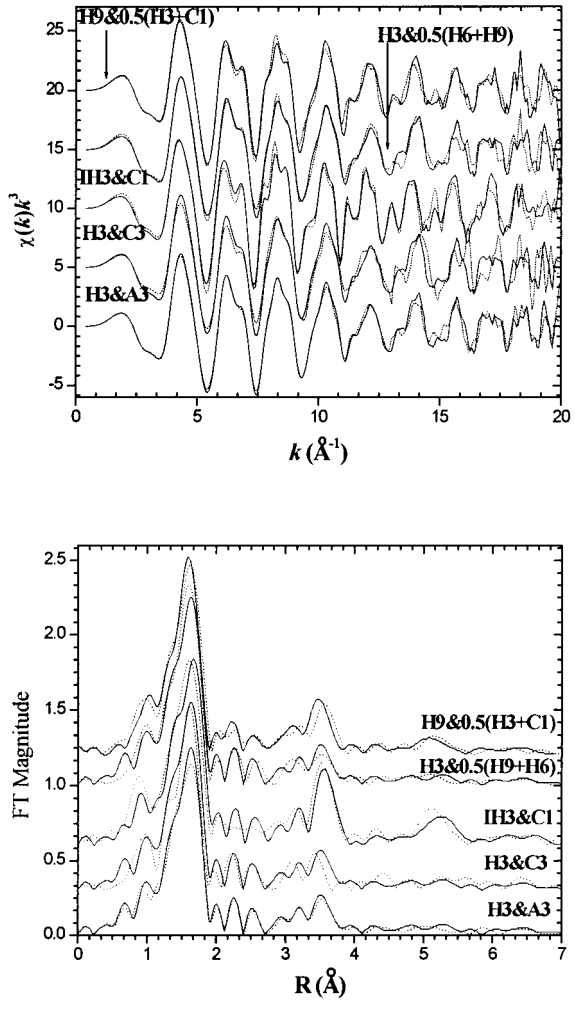

Figure 6. (a) Zr K-edge EXAFS and (b) Fourier transform magnitudes for a series of perovskite CZT samples. Data for a CZT 50/50 HSG sample are compared with those for materials prepared by reaction of oxides (H3 and C3) and the acetic acid route (H3 and A3). Data for a CZT 50/50 IHSG sample are compared with those for $CaZrO_3$ (IH3 and C1). Data for both CZT 50/50 and 75/25 samples are compared with weighted averages of the data for 75/25 and 25/75 (H3 and 0.5H6 + 0.5H9), and 100/0 and 50/50 (H9 and 0.5C1 + 0.5H3), respectively. In each case, the solid line corresponds to the first listed sample.

more of the samples used in the comparison is not a random solid solution or the assumption that the geometry of the Zr−O−Zr and Zr−O −Ti links are independent of solid-solution composition is unreasonable. A similar comparison between the FTs for sample H9 (CZT 75/25) and a weighted average of the spectra for H3 (50% CZT 50/50) and C1 (50% CZ) showed a discrepancy in the Zr−O−M region that is probably significant.

Influence of Processing Method on Solid-Solution Homogeneity. A comparison of the FTs for all the high-temperature CZT(50/50) samples is informative (see Figure 6b). The FTs and EXAFS for samples H3 and A3 are almost identical, indicating that the different processing chemistries lead to no significant variations in local structure. However, both the FT and EXAFS for IH3 differ markedly from those of H3. In fact, they strongly resemble those for $CaZrO_3$ (C1). This is consistent with the XRD data, which indicates that the

sample (IH3) is a mixture of $CaZrO_3$ and $CaTiO_3$.

Surprisingly, a comparison of the Zr K− edge EXAFS for a material prepared by high-temperature direct reaction of oxides (C3) with those for a sample prepared using alkoxide sol−gel chemistry (H3) (see Figure 6) shows some differences that are probably significant. In particular, the peak at ∼3.6 Å is shifted to slightly shorter distances for sample C3. On the basis of our FEFF7[34] simulations of the EXAFS for various CZT structural models, we believe that the shift in peak position that is observed indicates that the zirconium in the sol−gel CZT sample has more zirconium nearest neighbors than the zirconium in the other sample. This can be interpreted in several different ways. Either the material prepared by the direct reaction of oxides is displaying some short-range ordering of the titanium and zirconium or the sol−gel sample is a nonrandom solid solution that shows a preference for zirconium around zirconium or both of these phenomena are present simultaneously. We can exclude the possibility that the material prepared by the high-temperature reaction of oxides has a long-range ordered arrangement of titanium and zirconium as a Rietveld fit to the diffraction data using a random solid-solution model was very good and there were no extra peaks in the diffraction pattern.

Quantitative Analysis of the Zr−O EXAFS. During the analyses of the Zr−O EXAFS data, it was found that the one subshell 6-coordinate model only gave an adequate fit to the data for samples H3, A3, IH3, C3, H6, and H9, but the 2 + 2 + 2 model gave a good fit to all the data. Apparently, the distribution of Zr−O distances in the samples that had only been heated to low temperatures (H1, H2, IH1, IH2, A1, and A2) was too wide to fit with a single shell. An examination of the structural parameters obtained from the fitting (Table 2) for the materials prepared using alkoxide sol−gel chemistry indicated that the average Zr−O distance decreased slightly (from 2.12 to 2.09 Å) as the samples were heated to higher temperatures. While the significance of this decrease might be questioned, the larger decrease observed for the AAM materials (from 2.18 to 2.08 Å) is undoubtedly significant.

We have previously observed a change in apparent average Zr−O bond length of this magnitude upon heating ZrW_2O_8 dry gels that had been prepared using nonhydrolytic sol−gel chemistry.[63] A decrease in the average bond length is unreasonable if the zirconium in each sample is really coordinated by only six oxygen atoms, as was assumed during the modeling, as it would imply an increase in valence for the central zirconium atom.[64−66] However, it is entirely consistent with a reduction in coordination number for zirconium as the gel is heated. The zirconium in the dry gel presumably has an average coordination number greater than six and the average approaches six as the sample is heated. A decrease in the average bond length is associated with the reduction in coordination number so that the bond valence sum rule is satisfied.[64−66]

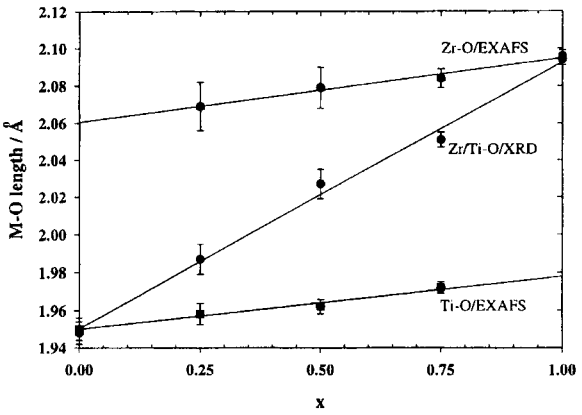

Figure 7. Comparison of the mean Zr/Ti−O distance determined by the Rietveld analysis of X-ray diffraction data for phase pure $CaZr_xTi_{1-x}O_3$ samples with the Zr−O and Ti−O bond lengths determined from the EXAFS data. In contrast to the M−O distances obtained by XRD, those from the EXAFS data only vary slightly with composition.

The observed differences between the local structures of the alkoxide and acetic-acid-derived CZT 50/50 dry-gel samples are not surprising as the chemistries of these two routes are markedly different. When acetic acid is added to titanium or zirconium alkoxides, the metals form chelates.[67,68] Infrared spectroscopy suggests that substitution reactions occur, resulting in the formation of species such as titanium isopropoxide acetate or zirconium propoxide acetate.[69] For PZT processed using an AAM method, it has been reported that no gel is formed, and stabilized titanium and zirconium species stay in solution when the molar ratio of acetic acid to metal is higher than 8.[70] Presumably, our CZT dry-gel powder prepared by the AAM route also contains species with coordinated acetate. The differences in chemistry also influence the crystallization of the resulting materials. The AAM xerogel contained no perovskite.

Comparison of the Diffraction and EXAFS M−O Distances. A full Rietveld analysis was performed for each of the CZT samples that had been prepared using the HSG procedure and heat-treated at 1200 °C for 20 h (samples H3, H6, and H9) and for both pure perovskite $CaTiO_3$ and $CaZrO_3$ (samples C1 and C2). The mean Zr/Ti−O distances that were obtained are plotted in Figure 7 and compared with the Zr−O and Ti−O bond lengths determined from the EXAFS data. The EXAFS values are almost independent of sample composition and only agree with those determined from the diffraction data for the solid-solution end members. The diffraction-derived values vary smoothly and markedly with sample composition. These differences arise because the EXAFS and diffraction experiments are fundamentally different. In a diffraction experiment, average atomic positions within the unit cell are determined and these average positions are used to calculate average bond lengths. The atomic positions are an

(63) Wilkinson, A. P.; Lind, C.; Pattanaik, S. *Chem. Mater.* **1999**, *11*, 101−108.
(64) Brown, I. D.; Wu, K. K. *Acta Crystallogr.* **1976**, *B32*, 1957−1959.
(65) Brown, I. D. *The Bond-Valence Method: An Empiracle Approach to Chemical Structure and Bonding*; Brown, I. D., Ed.; Academic Press: San Diego, CA, 1981; pp 1−30.
(66) Brown, I. D.; Altermatt, D. *Acta Crystallogr.* **1985**, *B41*, 244−247.
(67) Livage, J.; Henry, M.; Sanchez, C. *J. Phys. Solid State Chem.* **1992**, *18*.
(68) Doeuff, S.; Henry, M.; Sanchez, C.; Livage, J. *J. Non-Cryst. Solids* **1987**, *89*, 206−216.
(69) Yi, G.; Sayer, M. *J. Sol-Gel Sci. Technol.* **1996**, *6*, 65−74.
(70) Yi, G.; Sayer, M. *J. Sol-Gel Sci. Technol.* **1996**, *6*, 75−82.

average over all the unit cells in the sample and in a solid solution the unit cells are not all identical. In the EXAFS experiment, the bond lengths are a different kind of average. They are averages over all the Ti or Zr environments in the sample. The Zr−O and Ti−O bond lengths determined by EXAFS only change slightly with composition because their lengths are primarily determined by the bonding requirements of the metal and oxygen. The origin of the variation that is seen in our EXAFS-derived values is not clear. However, it may be associated with the strains that arise when trying to combine two different coordination polyhedra (TiO_6 and ZrO_6) in a somewhat disordered fashion to create a crystalline solid solution.

Conclusions

None of the solution routes investigated produced materials that crystallized as perovskite in a clean fashion, although for some of the samples perovskite was formed at <200 °C and pure perovskite was obtained upon heating at 1200 °C. Calcium-rich phases and a fluorite-related phase were observed in many of the samples along with perovskite at intermediate temperatures. The presence of the calcium-rich phase may be due to poor incorporation of the calcium into the polymer networks of the gels. While it is tempting to assume that the fluorite is zirconia-rich relative to the bulk sample composition, measurements of the perovskite lattice constants as a function of heat treatment conditions suggest that the fluorite has the same Zr/Ti ratio as the bulk sample. High titania content metastable fluorite phases have also been observed during the crystallization of sol−gel-processed PZT. The EXAFS and XANES data indicate that the local structures of the materials prepared by the alkoxide sol−gel and acetic-acid-modified routes are essentially identical after high-temperature heat treatment. For the other processing routes examined, there were indications that the route employed influences the compositional homogeneity of the solid-solution samples. The EXAFS and XANES data suggest that the coordination numbers of the Zr and Ti in the xerogels are different from those in the final perovskite products. The apparent preference of zirconium for a coordination number >6 and titanium for a coordination number <6 in the samples subjected to low-temperature heat treatment is probably a consequence of the significantly different ionic radii for these two ions (86 and 74.5 pm, respectively).

Supporting Information Available: Tables showing the dependence of the perovskite lattice constants on xerogel heat treatment conditions and the results of fitting the Ti XANES data. Figures showing the evolution of the XRD patterns upon heating the xerogels, the results of the TGA experiments, the fits to the Ti K-edge XANES data, the raw Zr K-edge XANES data, the effect of sample temperature on the quality of the EXAFS data, and a comparison of the EXAFS data for a CZT 50:50 xerogel with those for monoclinic zirconia. This material is available free of charge via the Internet at http://pubs.acs.org.

Acknowledgment. This work was primarily supported by NSF award DMR-9623890. The authors gratefully acknowledge the use of beamline X11A at the National Synchrotron Light Source, Brookhaven National Laboratory. X11A is supported, in part, by the U.S. Department of Energy, Division of Materials Science under Contract DE-FG02-89ER45384.

CM990774I